Environment, Development and Sustainability (2020) 22:661–692
https://doi.org/10.1007/s10668-018-0214-z

GIS and remote sensing-based analysis of the impacts of land use/land cover change (LULCC) on the environmental sustainability of Ekiti State, southwestern Nigeria

Idowu Ezekiel Olorunfemi[1] · Johnson Toyin Fasinmirin[1] · Ayorinde Akinlabi Olufayo[1,3] · Akinola Adesuji Komolafe[2]

Received: 7 April 2018 / Accepted: 30 June 2018 / Published online: 3 July 2018

Abstract
Analysis of land use/land cover change (LULCC) and their impacts on the natural environment is essential in policy decision for an effective solution to the sustainability of the earth system. This study employed supervised image classification (maximum likelihood) algorithm to map changes in land use/land cover for a period of 4.5 decades (1972–2017) in Ekiti State. Vegetation and temperature dynamics were examined for the selected years using normalized difference vegetation index (NDVI) and land surface temperature (LST), respectively. NDVI and LST were statistically compared to understand the potential impacts anthropogenic activities on the environment. Resultant LULC maps indicated a decrease in forests and woodlands at a change rate of 51.25 and 0.72% over the last 4.5 decades in Ekiti State, while built-up areas, croplands, rocks/bare soils and water bodies have increased about 267.58, 197.30, 714.11 and 4421.43%, respectively. Agricultural lands (now occupying 47.13%) are the major contributor to the net change in forests (decreasing). LST showed a negative correlation with NDVI ($r = -0.672$). Mean LST are in the order 22.7 °C (1984) < 23.84 °C (1991) < 27.17 °C (2017) < 28.16 °C (2000). As the LULC pattern is changing, its imprint is reflected on LST and NDVI. Built-up areas, rocks/bare soils exhibit the highest surface radiant temperature, while vegetated surfaces and water bodies recorded the least. The study demonstrated that changes in land covers through urban development have affected the natural functioning of ecosystems. As such, proper natural resource management and effective policies are required to ensure sustainable development.

Keywords Land use · Land cover · Land surface temperature · Normalized difference vegetation index · Sustainable environment

✉ Idowu Ezekiel Olorunfemi
olorunfemiidowu@gmail.com

[1] Department of Agricultural and Environmental Engineering, Federal University of Technology, Akure, Nigeria

[2] Department of Remote Sensing and Geoscience Information System, Federal University of Technology, Akure, Nigeria

[3] Department of Water Resources Management and Agro-meteorology, Federal University, Oye-Ekiti, Nigeria

1 Introduction

Most human activities take place on land and many materials required for such human activities come from it (Mengistu 2008). These anthropogenic activities are the main cause of LULCC (Weng 2001). Land use/land cover (LULC) consists of two separate concepts which are often used interchangeably (Rawat and Kumar 2015). Land use (LU) is any human purpose or intents applied to a specific portion of land commenced to effect a modification or maintain it (FAO/UNEP 1999). Land cover (LC), on the other hand, is the biological and physical state of the Earth's surface and the subsurface immediately below it (Wang et al. 2002). Land use/land cover change (LULCC) has been become one of the key elements in global environmental change and sustainable development (Wei et al. 2015). This is due to its pervasiveness on the local scale and its globally recognized environmental trend (Demessie 2015). Escalating agricultural and industrial activities brought about by rapidly increasing population have led to significant changes in LULC and greater demands on natural resources lodged in the land (Hegazy and Kaloop 2015).

A better understanding of landscape dynamics during a known period of time requires the detection of LULCC (Rawat and Kumar 2015). Researchers, planners and policy-makers utilize LULC information in evaluating urban growth patterns and determining changes in natural resources (Adeel 2010). Design of effective land management programmes requires proper knowledge of LULCC (Iqbal and Khan 2014). Unfortunately, lack of planning of LULCC due to human disturbances, changes in climate and rampant urban sprawl dynamics fueled by rapid population growth is the bane of most developing countries. These anthropogenic activities and influences on land include deforestation and overgrazing, industrial and residential zones (i.e., buildings, roads and other impervious surfaces), agricultural fields, logging and mining activities etc. (Zubair 2006). These changes in LULC also affects biodiversity, water and radiation budgets, trace gas emissions and other processes that come together to affect climate and biosphere (Rawat and Kumar 2015). Yet, LULCC detection is still the easiest detectable indicator of human influence on the land (Iqbal and Khan 2014). In the context of climate change and global warming, LULCC, especially deforestation and forest degradation contribute up to 20% of total net anthropogenic carbon emissions (Denman et al. 2007). They are the largest sources of carbon dioxide, methane and nitrous oxide emissions. As a result of these agricultural practices and changes in LULC, the global annual emission of carbon dioxide (CO_2) will increase (IPCC 2013). Such upsurge in the concentration of CO_2 causes about 50% of the total radiative forcing and will, consequently, aggravate the issue of climate change/global warming (IPCC 2013). In the light of this, quantifying LULCC and identifying its implications for the formulation of suitable targeted policy interventions is of utmost importance. This study, therefore, attempts to bridge science and policy gaps through innovation/outputs leading to more sustainable land management practices.

Rapid transformation of LULC has weighty impacts on human and natural environments (Dewan and Corner 2012). The increase in land surface temperature (LST) is one of such impacts (Pal and Akoma 2009). The land surface temperature, an estimate of actual ground temperature, is a major influence on physical processes responsible for the land surface balance of water, energy, and CO_2 (Kuenzer and Dech 2013). Due to its sensitivity to various land superficial features, LST has been used to extract information on diverse types of land uses/land covers (Ibrahim 2017). Higher solar radiation absorption, and a greater thermal capacity and conductivity are generally linked to urban areas resulting in elevated temperature commonly known as Urban Heat Islands (UHI) (Dewan and Corner

2012). As such, urban areas relatively experienced higher temperature as compared with surrounding rural areas (Weng 2001). Desertification, as a result of LULC modification, is another serious environmental and socio-economic problem occurring at all scales (global, regional and local) (Omran 2012). Many studies have applied normalized difference vegetation index (NDVI) in extracting vegetation abundance from remotely sensed data, and it has also been applied in indicating the extent of desertification by measuring features of vegetation cover (Higginbottom and Symeonakis 2014; Mohamed et al. 2011). Normalized difference vegetation index (NDVI) recompenses for changing illumination conditions, surface slope, and viewing angle and is therefore useful, especially, for monitoring vegetation from continental to global scale (USGS 2015). For mapping and monitoring the spatial distribution of LST (Voogt and Oke 2003) and NDVI, satellite remote sensing has proven to be an important data source (Babalola and Akinsanola 2016).

Ekiti State, Southwestern Nigeria over the past few decades have been witnessing rapid modification and alterations in the LULC through anthropogenic activities such as residential and institutional activities (NBS 2012). Overgrazing and deforestation as a result of expanding agricultural activities to meet up the fast-growing population are also prevalent (http://ekitistate.gov.ng, retrieved—2018, Feb. 6). Agricultural activities appear to be the dominant force responsible for major land transformations in the study area with the influx of other tribes from the Middlebelt (most especially the Igbiras from Kogi State and Igedes from Benue State) for farming activities. This is as a result of the high fertility status of soils in the State coupled with its favorable climatic condition (Olorunfemi et al. 2018). This has led to considerable increase in cultivated lands and development of several minor communities most especially in the northwestern part of the state. However, the continued expansion of the croplands and the increasing degradation of the forests for timbers and wood products for residential and institutional activities is not in tune with the ever-growing populations of the state (NBS 2012). There is also insufficient awareness among policy makers, planners and the general public to account for the multiple and often interacting determinants and impacts of LULCC in promoting sustainable land and environmental management.

Despite the increasing concerns about the impacts of LULCC on sustainable development and global changes of the environment (Wei et al. 2015), research on LULCC in southwestern Nigeria has just recently commenced. Most studies on LULCC are spatially concentrated in specific areas with major cities receiving attention on urban sprawl dynamics (Babalola and Akinsanola 2016; Ishola et al. 2016). However, availability, dynamics, and management of natural resources differ greatly temporarily and spatially (Veldkamp and Lambin 2001). Likewise, factors driving LULCC depend on the exact conditions of humans and their environments (Minta et al. 2018). In the study area, the magnitude and dynamics of these changes have not been extensively studied. Little is known about the spatiotemporal dimensions of the LULC changes that have modified and shaped the urban and agricultural expansion of Ekiti State (Olorunfemi 2014) and there is no complete information to evaluate LULC changes over time to improve selection of areas designated for agriculture, urban and/or industrial purposes (Rawat et al. 2013) in the region. In order to have a deep understanding of the aspects of change in the human–environment exchanges of a region at different time and space, numerous studies are required (Veldkamp and Verburg 2004).

To address this deficiency, the integration of remote sensing (RS) and geographical information system (GIS) data will provide great potential for uncovering, depicting, monitoring and assessment of LULCC and forest change (Kasischke et al. 2004). It is therefore of utmost importance to investigate LULCC so that its effect on the terrestrial ecosystem

can be detected, and sustainable land use planning can be devised (Muttitanon and Tripathi 2005). The present study will attempt to identify the spatiotemporal pattern of LULC changes for Ekiti State using geospatial data to enable decision makers to understand the dynamics of our changing environment and ensure sustainable development. Therefore, the objectives of this research are to quantify the spatiotemporal changes in land use and land cover between 1972 and 2017 in Ekiti State, evaluate changes in NDVI and LST of the study area for successive Landsat imageries of the study period (1972–2017) and assess the effect of LULCC on LST and NDVI.

2 Materials and methods

2.1 Study area

The study area, Ekiti State (Fig. 1), is located in the southwestern part of Nigeria. Ekiti State is located between Latitudes 7° 25′ to 8° 5′ N and Longitude 4° 45′ to 5° 45′ E and occupies a land area of about 5435 km^2 (NBS 2012). The State is mainly an upland zone with elevation ranging from 250 to 540 m above mean sea level (a.m.s.l.) (Simon-Oke et al. 2012). The State lies on an area underlain by metamorphic rock and is potentially rich in mineral deposits, which include channockete, limestone, kaolin, columbite, phosphate, iron ore, aquamine, gemstone, barite, gold among many others, largely deposited in different villages and towns within the study area (Olorunfemi and Fasinmirin 2017). Tropical climate exists in the State with two clear seasons [rainy season (April–October) and dry season (November–March)] (Olorunfemi and Fasinmirin 2017). High humidity

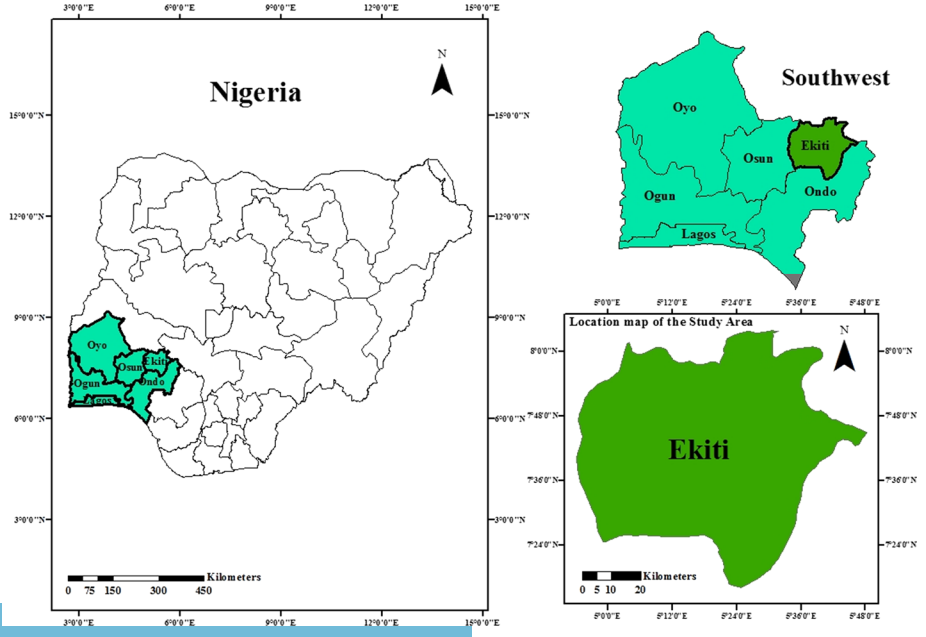

Fig. 1 Location of study area in the maps of Nigeria and Southwestern geopolitical zone of Nigeria

is being experienced in the state. Likewise, the mean air temperature ranges between 21 and 28 °C. Egbeda series and Iwo series are the dominant soils in Ekiti state (Smyth and Montgomery 1962), which under the FAO/UNESCO classification are classified as Orthic and Plinthic Luvisols, respectively (FAO 1998). Guinea forest vegetation with its attendant climate, flora, and fauna prevail in the State (Olorunfemi and Fasinmirin 2017). Derived savannah predominates exists in the north peripheries, while tropical rainforest predominates in the south (logbaby.com, retrieved—2018, Feb. 10). The study area includes both urban and rural components as well as vegetation and non-vegetation areas. Ekiti State has been experiencing a change in land use and land cover (LULC). The ever increasing population which numbered 1.63 million in 1991 grew to 2.38 million in 2006 with a projected population of 3.17 million in 2015 (ekitistate.gov.ng; citypopulation.de, retrieved—2018, Feb. 6). Ekiti State has a population density of 498.19/km^2 in 2015 subject to a change of +3.13% per year (2006–2015) (citypopulation.de, retrieved—2018, Feb. 6). This increase in human population has triggered many changes in the LULC of the study area.

2.2 Data acquisition and processing

This study employs Multispectral Scanner (MSS): Landsat Thematic Mapper (TM), Enhanced Thematic Mapper Plus (ETM+) and Operational Land Imager (OLI) satellite data to map and analyze the LULC change in the study area. Landsat MSS at a resolution of 60 m for the year 1972, TM for the years 1984 and 1991, ETM+ for the year 2000 and OLI for the year 2017 all at a resolution of 30 m were used for LULC classification (Table 1). Cloud–free Landsat images covering the study area (path 190, rows 054 and 055 with a spatial resolution of 60×60 m and 30×30 m) were obtained from the archives of United States Geological Survey (USGS) (Table 1). The two image scenes fell within the path/row: 190/054 and 190/055 of the worldwide reference system from which the data for the study location were extracted. Pre-processing of satellite images to extract meaningful data for easier interpretation was done (Iqbal and Khan 2014). To ensure spatial and temporal comparability of the datasets, the image pre-processing which include geometric and atmospheric corrections were performed in the geographic information system (GIS) environment (Hegazy and Kaloop 2015). Data were then pre-processed in ArcMap 10.5 for layer stacking, mosaicking and sub-setting of the image on the basis of Area of Interest (AOI).

2.3 LULC classification and analysis

Set of samples were created according to training samples which represent the desired land use types (Magidi 2010). These were used in the classification of the images. Training samples were selected by delineating polygons around characteristic sites for each of the predetermined LULC class (Butt et al. 2015). Ground-truthing, the researchers' personal experience and physiographical knowledge of the study area formed the basis of the training samples (Ishola et al. 2016). Band combination of 543 (Landsat 8 OLI), 432 (Landsat ETM+ and TM) and 321 (Landsat MSS) color composite images (vegetation) was prepared for visual interpretation and delineation of training areas (Fig. 2). Digitization of polygons around each training sample for the similar land cover was carried out using the chosen color composite. As such, a distinctive identifier was allotted to each known LULC type. Thereafter, statistical characterizations (i.e., signatures) of each LULC class (Ishola et al. 2016) were developed. Images

Table 1 Landsat metadata for the study area

State	Path/row	Satellite platform	Band used	%Cloud	Date acquired	Resolution (m)	Source
Ekiti	190/054; 190/055	Landsat MSS	321 (no thermal band)	1	12/03/1972	60	USGS
		Landsat 5 TM	432 and thermal band 6	0	11/12/1984	30	USGS
		Landsat 5 TM	432 and thermal band 6_1	0	05/01/1991	30	USGS
		Landsat 7 ETM+	432 and thermal band 6_2	0	15/02/2000	30	USGS
		Landsat 8 OLI	543 and thermal bands 10/11	0	04/01/2017	30	USGS

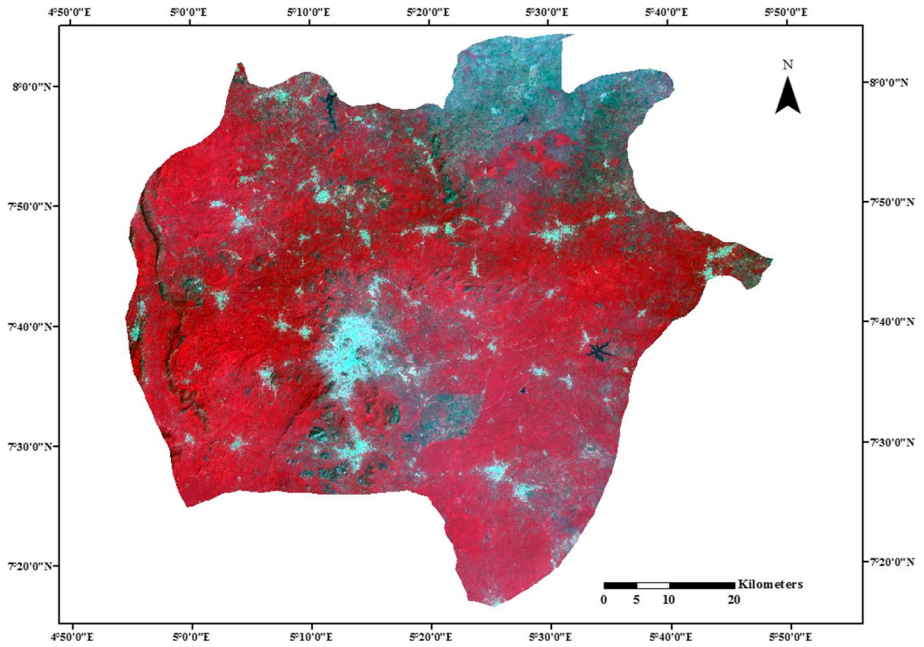

Fig. 2 Subset image of Landsat OLI 2017 (543 false color composite)

classification was then done using supervised classification approach. Maximum likelihood (MLH) algorithm for supervised classification of the images into different LULC categories (Lillesand and Kiefer 2007) was applied in ArcMap 10.5. Maximum likelihood algorithm is one of the most common classification methods when accurate training data are provided and one of the most widely used algorithms (Shalaby and Tateishi 2007). Maximum likelihood classification apart from considering the mean vector of the pixels in one class also accounted for the variability of these pixels in multispectral feature space (Kantakumar and Neelamsetti 2015). Since MLH is based on statistical parameters, it is considered to be one of the most accurate classifiers (Shalaby and Tateishi 2007). Based on control points using high-resolution Google Earth images and the GPS points, which were generated during fieldwork conducted between June and October, 2017, classified LULC using supervised classification was cross-checked with the ground truth points totaling 516 GPS points used for the classification. Photographs and GPS survey were carried out during the field experiments for sample points collection (June–October 2017).

For better classification results, normalized difference vegetation index (NDVI) was also applied to improve classification of the Landsat MSS images (explained by the relationship between visual resource of the NDVI and LULC types maps) at a resolution of 60 m of 1972 and Landsat TM images at a resolution of 30 m of 1984, 1991, 2000 and 2017. Six land use/cover types are identified and used in this study, namely (1) built-up areas (2) forests (3) croplands (4) woodlands (5) rocks/bare soils and (5) water bodies. More descriptions for the different LULC types and the reasons for grouping them are shown in Table 2.

Table 2 Classes delineated on the basis of supervised classification

Land use/land cover classes	General description
Built-up area	Commercial and residential buildings, industrial sites, construction sites, Institutional areas, roads and other man-made structures
Water bodies	Dams, Rivers, lakes, water reservoirs, ponds, and streams
Forests	Evergreen and Deciduous Broadleaf forests, medium and less dense forests
Croplands	Commercial and small-scale farms, irrigated and non-irrigated farms, fallow lands, sparsely vegetated lands
Rocks/Bare soils	Rocks, stone, hills, earth and sand land in-fillings, developed land, excavation sites, barren and bare lands
Woodlands	Closed and open woodlands, Shrubs, Woody Savannas and the remaining land cover types

2.4 Accuracy assessment

Classification accuracy denotes the degree of correspondence between remote sensing data and reference information (Iqbal and Khan 2014). Accuracy assessment of individual classification is important in assessing the practicality of classified data in change analysis detection (Owojori and Xie 2005). The accuracy assessment was carried out using ground truth points, based on ground truth data collected during the fieldwork, high-resolution Google Earth images and visual interpretation (Ishola et al. 2016). Error matrices were applied in the statistical comparison of reference data and classification results. The error matrices were generated to assess the user's accuracy, producer's accuracy, and overall classification accuracy. In addition, a nonparametric Kappa test was also performed to measure the extent of classification accuracy as it does not only accounts for diagonal elements but for all the elements in the confusion matrix (Minta et al. 2018). Kappa coefficient was calculated using Eq. (1):

$$K = \frac{N\sum_{i=l}^{r} X_{ii} - \sum_{i=l}^{r}\left(X_{i+} \times X_{+i}\right)}{N^2 - \sum_{i=l}^{r}\left(X_{i+} \times X_{+i}\right)} \tag{1}$$

where K = kappa coefficient, N = total number of values, $\pi \sum_{i=l}^{r} X_{ii}$ = observed accuracy and $\sum_{i=l}^{r}\left(X_{i+} \times X_{+i}\right)$ = chance accuracy.

2.5 LULC change detection and analysis

Change detection in the study was performed in ArcGIS 10.5 and Land Change Modeler (LCM) within Terrset to detect land use/cover change. Change detection was applied to compare and analyze the LULC maps that finally emerged between 1972 and 2017 as a result of visual interpretation and subsequent supervised classification (Butt et al. 2015). Images of the same scene at different times are being described and quantified by change detection technique. These classified images at different times were used to calculate the area (sq.km and %) of different land covers and also observe and identify changes occurring in different classes of LULC (Yuan et al. 1998) like an increase in urban built-up area or decrease in forests and so

on. Percent (%) change in the same LULC type between two-time interval is calculated using Eq. (2):

$$\text{Percent (\%) change} = \frac{A_x - A_{x-1}}{A_{x-1}} \times 100 \tag{2}$$

where A_x = area of specific LULC type at time x, A_{x-1} = area of specific LULC at time $x-1$

Land Change Modeler (LCM), a vertical application, within Tersset Geospatial Monitoring and Modeling System for sustainable development and biodiversity conservation was used for the analysis of the pattern and trend of change of LULC in the study area (Eastman 2016). The LCM is an innovative land planning and decision support tool, which allows rapid assessment of change and the formation of viable strategies and scenarios for future land change (Eastman 2016). The LCM allows us to evaluate the gains and losses, net change and specific transitions among LULC classes (Ishola et al. 2016). Using the LCM within Terrset, Net change (sq km) between two-time interval is calculated using Eq. (3):

$$\text{Net change (sq km)} = \text{Gains} - \text{Losses} \tag{3}$$

2.6 Normalized difference vegetation index estimation

Normalized difference vegetation index (NDVI), an index of vegetation abundance (Mohamed et al. 2011) was calculated for each available image. The NDVI is based on the difference between the maximum reflection of radiation in the near-infrared spectral bands (0.78–0.90 µm) and the maximum absorption of radiation in the red spectral band (0.63–0.69 µm) (Higginbottom and Symeonakis 2014).

Mathematically NDVI is calculated using Eq. (4) (Rouse et al. 1974):

$$\text{NDVI} = \frac{\text{NIR} - \text{Red}}{\text{NIR} + \text{Red}} \tag{4}$$

Values of the NDVI range between − 1.0 and + 1.0 (Higginbottom and Symeonakis 2014). NDVI is the most frequently used vegetation index for monitoring vegetation universally owing to its positive correlation with characteristics of plant status and abundance (Aldoski et al. 2013).

2.7 Retrieving land surface temperature

The LST was derived from the TM and ETM+ thermal infrared band (band 6) with a spatial resolution of 60 m and OLI thermal infrared bands 1 and 2 (average of bands 10 and 11). Acquired TIRS bands at 100 m resolution were resampled to 30 m in delivered data product.

2.7.1 Land surface temperature retrieval

The LST was calculated using Eq. (5) proposed by Artis and Carnahan (1982):

$$\text{LST} = \frac{T}{1 + w \times \left[\left(\frac{T}{p}\right) \times \ln(e)\right]} \tag{5}$$

where T = at-satellite brightness temperature, w = wavelength of the emitted radiance of the thermal infrared band (Markham and Barker 1985) used and, e = land surface emissivity (0.99–1.01)

$$p = \frac{h \times c}{s\left(1.438 \times 10^{-2}\text{m K}\right)} \tag{6}$$

where h = Planck's constant (6.626×10^{-34} Js) c = velocity of light (2.998×10^{8} m/s), s = Boltzmann constant (1.38×10^{-23} J/K),

2.7.2 Conversion of the digital number (DN) to TOA spectral radiance (L_λ)

First, the digital number (DN) values were converted to spectral radiance by means of reference values (radiant rescaling factors provided in the metadata) by the following Eq. (7) (Landsat Project Science Office 2002):

$$L_\lambda = M_L Q_{\text{cal}} + A_L \tag{7}$$

where L_λ = spectral radiance (W/(m^2 × srad × μm)), M_L and A_L are band-specific multiplication and additive rescaling factors which can be acquired from the header file of the images. Q_{cal} is the digital number (DN) (Quantized and calibrated standard product pixel values).

2.7.3 Conversion of spectral radiance (L_λ) to at-satellite brightness temperature (T)

The spectral radiance was then transformed to At-satellite brightness temperature using the thermal constants provided in the metadata file by the following Eq. (8) (Artis and Carnahan 1982):

$$T = \frac{K_2}{\ln\left(\frac{K_1}{L_\lambda} + 1\right)} \tag{8}$$

where T = at-satellite brightness temperature (K), K_2 and K_1 are band-specific thermal conversion constants (calibration constants) and L_λ = spectral radiance (W/(m^2 × srad × μm)) K_1 = 607.76/666.09 and K_2 = 1260.56/1282.71 (Wm^{-2} sr^{-1} μ m^{-1}) for band 6 of Landsat 5/7. K_1 = 174.85/480.89 and K_2 = 1321.08/1210.14 (Wm^{-2} sr^{-1} μ m^{-1}) for bands 10 and 11 of Landsat 8. For this study, an average of TIRS bands 10 and 11 was used.

2.7.4 Deriving land surface emissivity (LSE)

The calculation of land surface emissivity (LSE) is critical to the retrieval of LST.

LSE (e) is calculated using Eq. (10) (Landsat Project Science Office 2002; Pal and Ziaul 2015). First, we calculate the proportion of vegetation (P_v) (Eq. 9) (Pal and Ziaul 2015):

$$P_v = \left(\frac{\text{NDVI} - \text{NDVI}_{\text{min}}}{\text{NDVI}_{\text{max}} - \text{NDVI}_{\text{min}}}\right)^2 \tag{9}$$

$$e = \left(0.004 \times P_v\right) + 0.986 \tag{10}$$

2.7.5 Conversion of LST from Kelvin to degree Celsius

After the emissivity corrected land surface temperatures were estimated in degrees Kelvin, for easy comprehension, the above derived LSTs' unit was converted to degree Celsius using the relation of 0 °C equals 273.15 K. The temperature values were thereafter converted to degrees Celsius by simply subtracting 273.15 using the relation:

$$\mathrm{LST}(^{\circ}\mathrm{C}) = \mathrm{LST}(^{\circ}\mathrm{K}) - 273.15 \tag{11}$$

3 Results

3.1 Land use/land cover classification

The land cover classification maps of the years under study—1972, 1984, 1991, 2000 and 2017 is presented in Fig. 3. LULC maps were generated from supervised classification of satellite images (Fig. 3). The satellite image of the years studied was categorized into six classes, i.e., built-up areas (BA), forests (FOR), croplands (CP), woodlands (WD), rocks/bare soils (RB) and water bodies (WB) (Fig. 3). The data obtained through the analysis of multi-temporal satellite imageries are diagrammatically illustrated in Fig. 4.

Accuracy assessment was carried to assess the practicality of classified data in change analysis. For accuracy assessment, the producer's accuracy, user's accuracy, overall accuracy and kappa statistics were calculated for the year 2017 image by generating error matrices (Table 3). The overall classification accuracy assessment and Kappa statistics of the LULC information derived from Landsat OLI scenes were 92.83 and 90.87%, respectively (Table 3). This level of accuracy conforms with the standard accuracy of > 90% for LULC mapping studies recommended by Lea and Curtis (2010).

LULC mapping shows that forests cover 3871.99 km^2 (73.90%), built-up areas occupy 25.68 km^2 (0.49%), while 831.25 km^2 (15.85%) falls under croplands. Likewise, woodlands occupy 474.26 km^2 (9.04%), rocks/bare soils cover 37.48 km^2 (0.71%), while the remaining area falls under water bodies 0.14 km^2 (0.003%). Similarly, the classification results (Fig. 4) of 2017 reveal that forests, built-up areas, croplands, woodlands, rocks/bare soils and water bodies occupy 36.04% (1888.80 km^2), 1.80% (94.57 km^2), 47.10% (2468.51 km^2), 9.12% (478.07 km^2), 5.81% (304.72 km^2) and 0.12% (6.33 km^2) of the study area, respectively. Considering area distribution values (Table 4) for land use/land cover for the years 1972, 1984, 1991, 2000 and 2017, it was observed that forests occupied the largest area extents in 1972 (73.90%), 1984 (63.56%), 1991 (58.68%) and 2000 (42.61%) but by the year 2017, croplands has overtaken forest by occupying an estimated 47.10% of the study area. On the other hand, water bodies occupied the smallest area in the year 1972 (0.003%), 1984 (0.18%), 1991 (0.14%), 2000 (0.13%) and 2017 (0.12%).

3.2 Land use and land cover dynamics (1972–2107)

The LULC changes resulting from the comparison of classified Landsat images of 1972, 1984, 1991, 2000 and 2017 are presented in Tables 4 and 5. Spatial patterns of LULC changes are shown in Fig. 4. We observed that both positive and negative changes occurred in the LULC pattern of Ekiti State. The LULC changes that occurred between 1972–1984, 1984–1991, 1991–2000, 2000–2017, 1972–1991, 1972–2000, 1984–2000, 1972–2017,

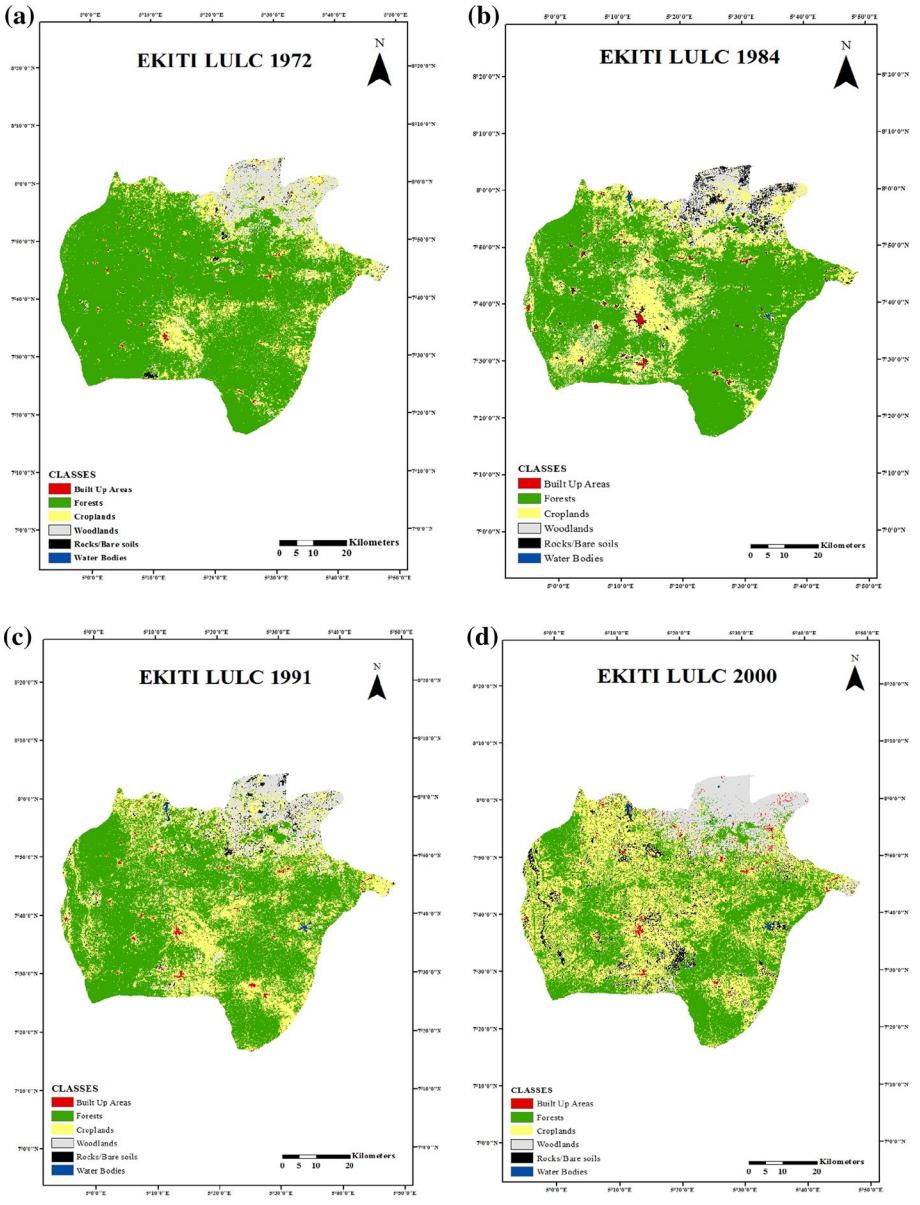

Fig. 3 The classified maps of Ekiti State for the study period **a** 1972, **b** 1984, **c** 1991, **d** 2000 and **e** 2017

1984–2017 and 1991–2017 are presented diagrammatically (Figs. 5, 6). In 1972, forests dominated the entire landscapes covering a total of 73.90% of the total study area (5238.75 km^2). However, progressive decrease in areas covered by forest was observed in the analysis of five periods of time (1972–1984–1991–2000–2017) which could be attributed to the expansion of croplands. By 2017, cropland has become the principal land use type occupying 47.13% (more than one-third) of the total area while forest now covers

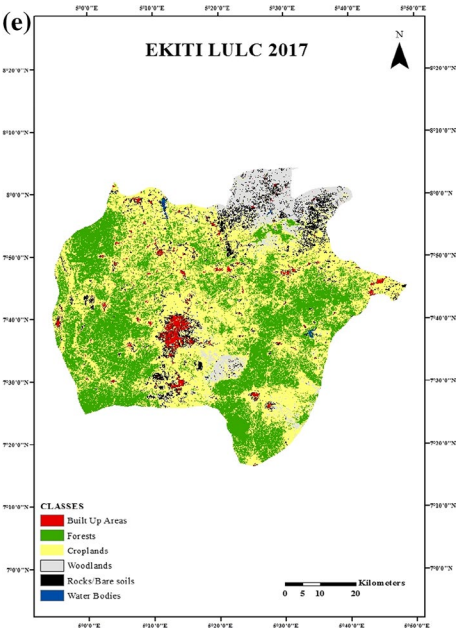

Fig. 3 (continued)

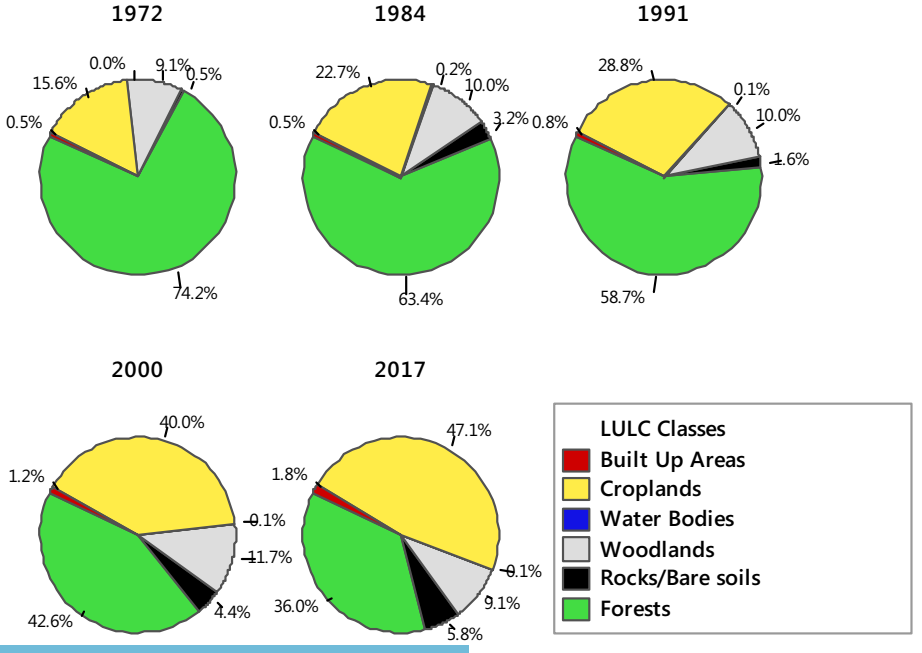

Fig. 4 Percentage distribution of LULC Classes of the study area

Table 3 Classification accuracy assessment for the year 2017

Predicted LULC type	BA	FOR	CP	WD	RB	WB	Row total	Producer's accuracy (%)	User's accuracy (%)
BA	125	0	0	0	4	0	129	96.90	96.15
FOR	0	130	4	3	0	0	137	94.89	99.24
CP	2	1	122	7	3	0	135	90.37	93.85
WD	0	0	4	33	2	0	39	84.62	70.21
RB	3	0	0	4	21	0	28	75.00	70.00
WB	0	0	0	0	0	48	48	100.00	100.00
Column total	130	131	130	47	30	48	516		
Overall classification accuracy = 92.83%, Kappa Coefficient = 90.87%									

36.03% (Table 4 and Fig. 4). Over the entire period of study (1972–2017), the coverage of built-up areas, croplands, woodlands, rocks/bare soils and water bodies increased by 267.58, 197.30, 0.72, 714.11 and 4421.43%, respectively, while forest declined by 51.25% (Fig. 6).

Land use/land covers varied distinctively in areas during the intervals of the period of study (Table 5). Built-up areas expanded at a moderate annual rate of 2.4% between 1972 and 1984 but increases to 3.6% per annum growth rate between 1984 and 1991 (Table 5). There was a fast-tracked development of BA between 1991 and 2000 at an annual rate of 5.8% but the rate of development in the building sector decrease to 2.9% per annum between 2000 and 2017 which might not be unconnected to the dwindling economic fortune of the state. As at 1972, FOR occupied close to four fifths of the entire state (3871.23 km^2), but by the year 2017, it has been reduced to 1887.28 km^2 (less than two-fifths) of the state (Table 4). Deforestation rate was highest in the interval of 1991 to 2000 at a rate of 3.1% per annum (Table 5). However, deforestation rate in the last period of the study appeared to have dropped to 0.9% per annum, but the degradation of the forest is still a major issue to combat. Increasing agricultural activities fueled by the rapid population growth (as seen in 5.8% annual growth rate of BA between 1991–2000) are the major cause of deforestation during this period. In addition, increasing degradation of the forests for timbers and wood products for residential and institutional activities also played major roles in the deforestation and forest degradation activities. Prevalent activities of charcoal merchants in the northwestern part of the state have equally contributed to the alarming rate of deforestation and forest degradation witnessed in the state. The activities of illegal loggers in the state and forestry officers/guards scheming with timber contractors to perpetrate illegalities have led to the immense loss of several indigenous trees and forests most especially the rosewood (*Pterocarpus erinaceus*), locally known as Kosso and other tree species which has accentuated the depletion of the state's forestry resources. Currently, the state government in a bid to conserve the remaining native trees and forests in the state is working with the legislative arm of the government to enact a law prohibiting the illegal and chaotic felling of trees.

Croplands, like built-up areas, increase considerably at annual rates of 2.8, 5.1 and 4.3% in periods 1972–1984, 1984–1991 and 1991–2000, respectively (Table 5). However, the annual rate of expansion of CP between 2000 and 2017 was not as significant as the previous periods probably due to the labor intensive associated with the agricultural sector.

Table 4 Land use/land cover classes of the study areas (Sq. km)

LULC CLASSES	1972		1984		1991		2000		2017	
	Area (Sq. km)	Area (%)	Area (Sq. km)	Area (%)	Area (Sq. km)	Area (%)	Area (Sq. km)	Area (%)	Area (Sq. km)	Area (%)
Built-up areas	25.66	0.49	33.00	0.63	41.41	0.79	62.84	1.20	94.32	1.80
Forests	3871.23	73.90	3329.56	63.56	3076.14	58.72	2231.40	42.59	1887.28	36.03
Croplands	830.48	15.85	1112.73	21.24	1506.82	28.76	2094.65	39.98	2469.00	47.13
Woodlands	473.83	9.04	580.39	11.07	524.20	10.01	610.66	11.66	477.26	9.11
Rocks/bare soils	37.41	0.71	173.87	3.32	82.82	1.58	232.52	4.44	304.56	5.81
Water bodies	0.14	0.003	9.43	0.18	7.36	0.14	6.69	0.13	6.33	0.12
Total	5238.75	100.00	5238.75	100.00	5238.75	100.00	5238.75	100.00	5238.75	100.00

Table 5 Changes in LULC for the periods 1972–1984, 1984–1991, 1991–2000, 2000–2017

LULC	Percent (%) change					Annual rates of changes			
	1972–1984	1984–1991	1991–2000	2000–2017	1972–2017	1972–1984	1984–1991	1991–2000	2000–2017
Built-up areas	28.60	25.48	51.75	50.10	267.58	2.4	3.6	5.8	2.9
Forests	−13.99	−7.61	−27.46	−15.42	−51.25	1.2	1.1	3.1	0.9
Croplands	33.99	35.42	39.01	17.87	197.30	2.8	5.1	4.3	1.1
Woodlands	22.49	−9.68	16.49	−21.85	0.72	1.9	1.4	1.8	1.3
Rocks/bare soils	364.77	−52.37	180.75	30.98	714.11	30.4	7.5	20.1	1.8
Water bodies	6635.71	−21.95	−9.10	−5.38	4421.43	553.0	3.1	1.0	0.3

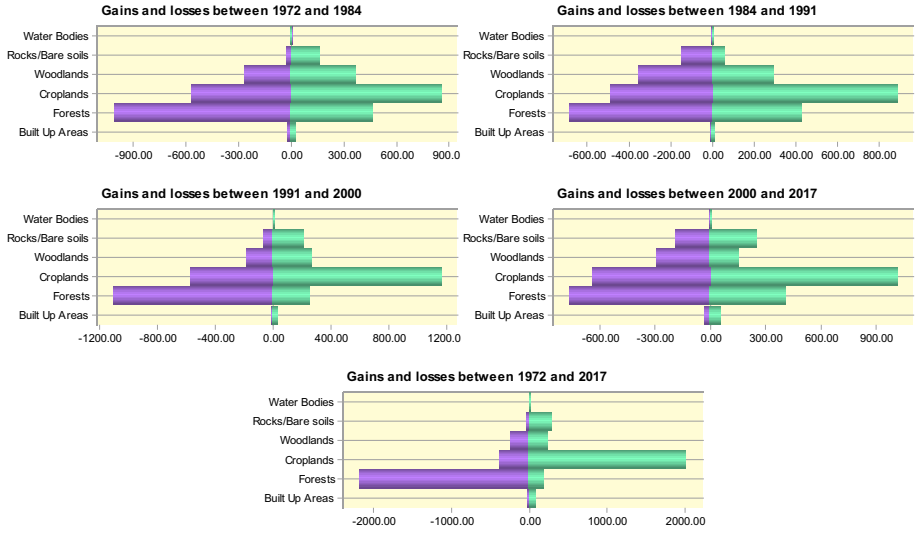

Fig. 5 Net losses and gains per specified period

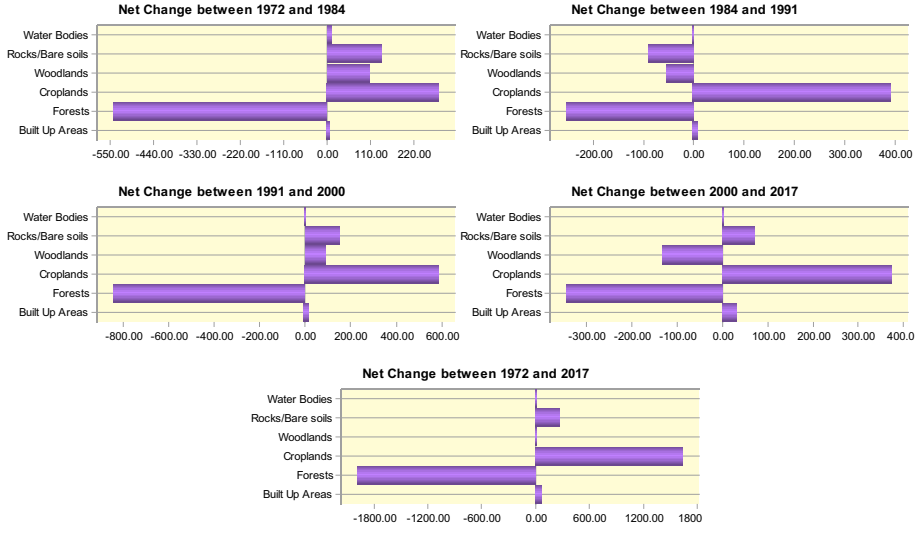

Fig. 6 Net change (sq km) per specified period

For close to two decades, i.e., 2000–2017, BA in the study area increased from 62.84 to 94.32 km^2, while CP equally increased from 2094.65 to 2469.00 km^2. Whereas FOR decreased from 2231.40 km^2 in 2000 to 1887.28 km^2 in 2017. Woodlands among the various LULC did not experience a remarkable net change in the 45 years of study. There was no obvious trend in the changes observed in the woodlands as both increment and reduction were observed. Water bodies in the periods 1972–1984 witnessed an increase in its coverage over the state (6635.71%) at an unexpected rate of 553% per annum (Table 5).

The unexpected expansion in WB in the state between 1972 and 1984 is not unconnected to the construction of 3 large dams (Itapaji dam, Egbe dam and Ero Dam), respectively. Presently, there four dams located in the study area but as at 1972 (when the first satellite image, MSS, was acquired), only one of the dams (Ureje Dam), a small earth/concrete dam constructed in the year 1958 was in existence. The construction of the three large dams was completed in the years 1975, 1983 and 1985. In the remaining periods, 1984–1991, 1991–2000 and 2000–2017, the coverage of water bodies declines unlike the period before (1972–1984), at 3.1, 1 and 0.3%, respectively (Table 5).

3.3 Trends in transition between land use/land covers

Figure 5 of gains and losses in coverage of LULC class in periods 1972–1984, 1984–1991, 1991–2000, 2000–2017 and 1972–2017 reveals that 1010. 99, 684.27, 1101.09, 761. 84 and 2181.41 km^2 FOR coverage were lost to other LULC classes. In a long-time period of four and half decades (1972–2017), about 57% of FOR were lost to other LULC classes implying that more than half of the existed FOR coverage were modified to other LULC types. In all the periods under consideration, FOR lost more than it gained, a big threat to biodiversity as such scenario has caused immense loss of several indigenous trees which has accentuated the depletion of the state's forestry resources and extinction of several species. On the contrary, significant gains were recorded in the coverage of croplands and built-up areas over the entire landscapes in the periods. These LULC categories in each time period gained more than they lost. The long period analysis between 1972 and 2017 showed that CP had gained a total of 2023.13 km^2 coverage of the entire landscape while losing only 384.66 km^2 (Fig. 5). There was no obvious trend in the gains and losses experienced by woodlands and rocks/bare soils in the time periods (Fig. 5). Forest land cover class was subjected to significant and regressive change in all periods as shown in Fig. 6 of the net change analysis in the various LULC classes. Forests are continually being depleted due to the felling of valued indigenous trees for timber products with no provision to replant (Ogundare 2016). Such activities eventually opened up the forest for croplands to take over. Croplands, on the other hand, showed an increasing net change in all the time periods (Fig. 6) as farmers go on the search of virgin lands year in year out due to its high nutrients composition. The allegations that the consumption of agricultural produce from fertilizers enhanced soils causes a variety of diseases and that the use of herbicides in controlling weeds degrade lands is partly responsible for the increasing expansion of croplands. This cultural attitude on the part of the farmers fueled their sustained practices of shifting cultivation and the bush burning method of land clearing leading to zone farming annually in the state (Ogundare 2016), thus expanding coverage of croplands.

Table 6 of the conversion pattern between the various LULC categories in the period 1972–2017 within the state. The transition established the patterns of LULC changes and the contribution of a specific land cover class to the change witnessed in another class. We observed that in all periods between 1972 and 2017, CP is the major contributor to the net change in FOR (decreasing) as FOR was a major source of land cover conversion to CP. Another good source of land conversion to CP is the woodlands. This further revealed that agricultural activities are the major driver of deforestation in the state. However, WB was not in perceptible anyway converted to CP. The decrease in the amount of FOR converted to CP in the last period (2000–2017) is due to the gradual downward trend in agricultural practices among the locals. Drudgery involves in farming activities without conventional farming implements (Ogundare 2016) and aging of the earlier generation of locals involved

Table 6 Transitions between major LULC between 1972 and 2017, Ekiti State, Nigeria

LULC	LULC (2nd ref. year)						Total (km^2)
	BA (km^2)	FOR (km^2)	CP (km^2)	WD (km^2)	RB (km^2)	WB (km^2)	
1972–1984							
BA	*4.47*	13.18	4.01	1.50	2.50	0.00	25.66
FOR	18.36	*2860.23*	708.36	238.50	42.49	3.29	3871.23
CP	9.05	391.08	*256.20*	122.69	48.16	3.29	830.48
WD	0.74	54.64	138.37	*205.25*	72.55	2.28	473.83
RB	0.38	10.38	5.72	12.19	*8.17*	0.57	37.41
WB	0.00	0.04	0.07	0.02	0.00	0.00	0.14
Total (km^2)	33.00	3329.56	1112.73	580.15	173.87	9.43	5238.73
1984–1991							
BA	*26.44*	0.01	6.47	0.06	0.01	0.00	33.00
FOR	0.28	*2645.29*	644.37	38.29	1.33	0.00	3329.56
CP	3.20	284.32	*620.35*	183.56	21.02	0.28	1112.73
WD	0.40	143.00	174.35	*225.29*	36.84	0.27	580.15
RB	11.09	3.51	60.54	75.43	*22.50*	0.79	173.87
WB	0.00	0.00	0.73	1.56	1.13	*6.01*	9.43
Total (km^2)	41.41	3076.14	1506.82	524.20	82.82	7.36	5238.75
1991–2000							
BA	*25.25*	0.03	15.29	0.70	0.13	0.00	41.41
FOR	1.38	*1975.05*	1038.57	23.63	37.52	0.00	3076.14
CP	25.31	229.59	*930.59*	189.10	132.17	0.07	1506.82
WD	8.99	24.46	102.88	*338.69*	48.98	0.20	524.20
RB	1.90	2.26	7.28	58.30	*12.83*	0.25	82.82
WB	0.01	0.01	0.04	0.24	0.88	*6.17*	7.36
Total (km^2)	62.84	2231.40	2094.65	610.66	232.52	6.69	5238.75
2000–2017							
BA	*30.93*	0.02	11.91	5.86	14.12	0.00	62.84
FOR	1.31	*1469.56*	708.53	40.85	11.14	0.01	2231.40
CP	51.96	408.49	*1454.52*	78.26	101.38	0.04	2094.64
WD	4.52	1.65	154.10	*317.00*	133.31	0.08	610.66
RB	5.59	7.54	139.93	34.94	*44.21*	0.30	232.52
WB	0.00	0.01	0.00	0.36	0.42	*5.90*	6.69
Total (km^2)	94.32	1887.28	2469.00	477.26	304.57	6.33	5238.75
1972–2017							
BA	*5.65*	6.70	10.13	1.27	1.90	0.01	25.66
FOR	54.03	*1689.82*	1879.52	125.99	118.56	3.30	3871.23
CP	29.23	161.15	*445.82*	111.06	80.87	2.35	830.48
WD	4.61	23.63	123.90	*226.55*	94.81	0.33	473.83
RB	0.79	5.98	9.56	12.39	*8.36*	0.33	37.41
WB	0.00	0.01	0.06	0.00	0.06	0.00	0.14
Total (km^2)	94.31	1887.28	2469.00	477.25	304.56	6.33	5238.75

Italic values represent persistence of LULC type

in farming practices explains in part the reason for the decline in practices and productivity. Also, the cultural attitude of the younger generation toward farming practices could somewhat be responsible for this decline. More importantly poor pricing policy, low access to agricultural credit, land tenure system and degradation and poor market access and marketing efficiency are the major constraints facing the agricultural sector in recent times. Between 2000 and 2017, more than 408 km^2 of croplands were converted to secondary forests (Table 6) probably due to the restoration of soil fertility through a fallow system of farming employed by the locals.

3.4 Normalized difference vegetation index (NDVI) of the study area

Normalized difference vegetation index (NDVI), an index based on spectral reflectance of the ground surface feature of near-infrared and red bands is commonly used to monitor the condition of vegetation or vegetation health (Al-doski et al. 2013). In this study, the NDVI value calculated from Landsat satellite image of the year 1972 varies from 0.79 to −0.15, 1984 NDVI value ranges from 0.54 to −0.33 while that of 1991 ranges from 0.47 to −0.18 showing a decrease in the NDVI values (Fig. 8). There was a further reduction in the highest NDVI values for the year 2017 with the NDVI ranging from 0.39 to −0.01. Comparing the NDVI values of the years 1972, 1984, 1991, 2000 and 2017, we observed a significant change across the whole study area with a corresponding change in the highest NDVI values (Fig. 7). The spatial pattern of the NDVI distribution shows that vegetated areas have high NDVI values relative to non-vegetated areas (Fig. 8).

3.5 Land surface temperature (LST) of the study area

LST maps from the acquired Landsat imageries were used to analyze the relationship between LULC types and surface temperature. The LST maps for successive Landsat imageries of 1984, 1991, 2000 and 2017 showed the change in intensity of LST over the time periods (Fig. 9). The absence of a thermal infrared band in the 1972 Landsat Multispectral Scanner made it impossible to retrieve the land surface temperature for that year. The land surface temperature of the year 1984 varied from 18.93 to 45.45 °C with an average value of 22.7 °C (±1.65), while LST of 1991 Landsat image varied from 20.47 to 44.59 °C with a mean value of 23.84 °C (±1.38). LST of 2000 Landsat image has classification statistics of minimum, maximum and mean

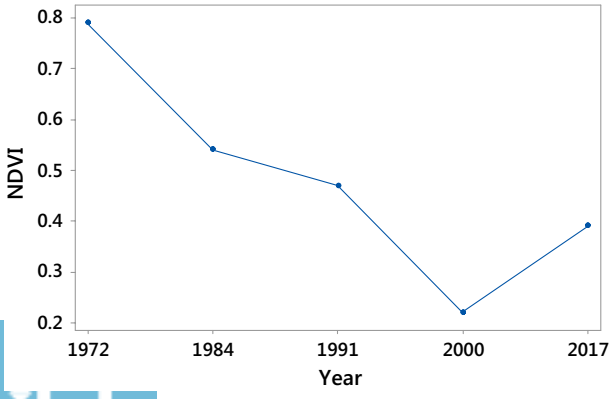

Fig. 7 Trend of NDVI Upper Values from 1972 to 2017

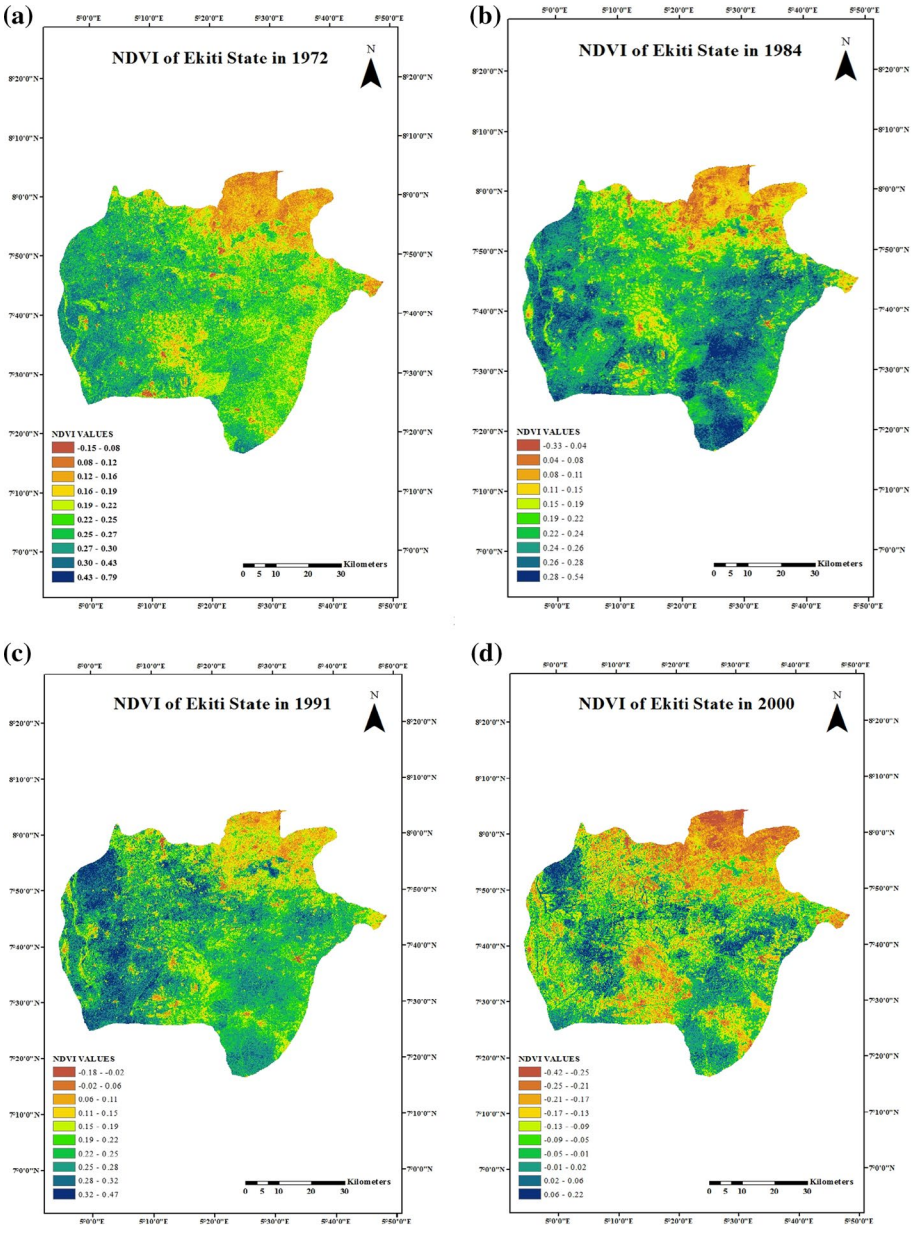

Fig. 8 NDVI maps of Ekiti State for the years **a** 1972, **b** 1984, **c** 1991, **d** 2000 and **e** 2017

values of 21.84, 49.94, and 28.16 °C (±2.44). Likewise, 2017 Landsat image recorded land surface temperature ranging from 23.04 to 41.64 °C with an average value of 27.17 °C (±1.99). Mean LST values are in the order 22.7 °C (1984) < 23.84 °C (1991) < 27.17 °C (2017) < 28.16 °C (2000). Human activities like the modification of LULC classes resulting from rapidly increasing population might have caused the increasing

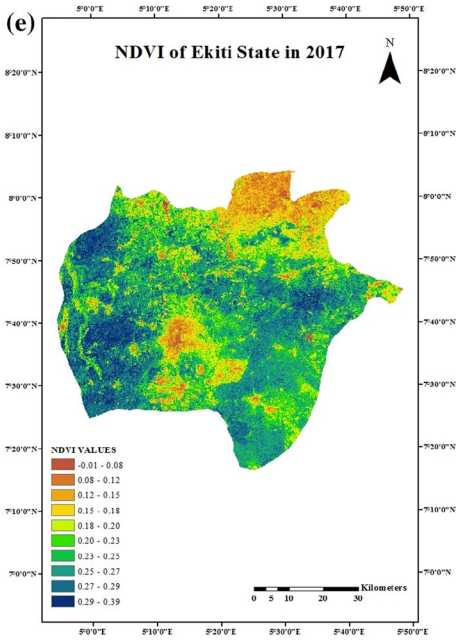

Fig. 8 (continued)

trend of LST over the landscape (Mallick et al. 2008). The LST map of 2017 Landsat image was found to have more areas with distinct red colors (urban areas, rock outcrops and uncultivated bare land) signifying high land surface temperature (Pal and Akoma 2009) with a temperature range of 35–42 °C, while the reverse was noticed in the LST map of 1984 as very few areas showed element of high surface temperature.

Figure 12 shows the changing pattern of LST zones in periods 1984–2017 in the study area. Very few insignificant areas experienced extreme temperature (≥ 41 °C) in all periods when the satellite over passed (Figs. 9, 12). The percentage temperature zones of the entire area fell into the following categories in 1984; < 25 °C (87.10%), 25 to < 30 °C (12.78%), 30 to ≤ 40 °C (0.12%) of lower, middle and high categories of temperature zones, respectively. We observed that majority (87.10%) of the areas fall in the lower categories of temperature zone in 1984 (Fig. 12). In 1991, a considerable 75% of the total area fall under the low temperature zone (< 25 °C), while 25.24 and 0.1% were found in the middle and high temperature zones, respectively. However, in 2000 and 2017, the majority of the area (81.93 and 88.85%) were dominated by the middle temperature zone (25 to < 30 °C), respectively.

The percentage in the high temperature zone (30 to ≤ 40 °C) were equally higher relative to the previous two periods (1984 and 1991) as other surface areas (15.58 and 8.67%) fell in the high temperature zone in 2000 and 2017 periods of study, respectively (Fig. 12). The few percentage of land areas falling under the high temperature zones might be as a result of the hilly terrain of the area resulting in large expanse of impervious areas from which the state derived her name "Ekiti" meaning hilly state.

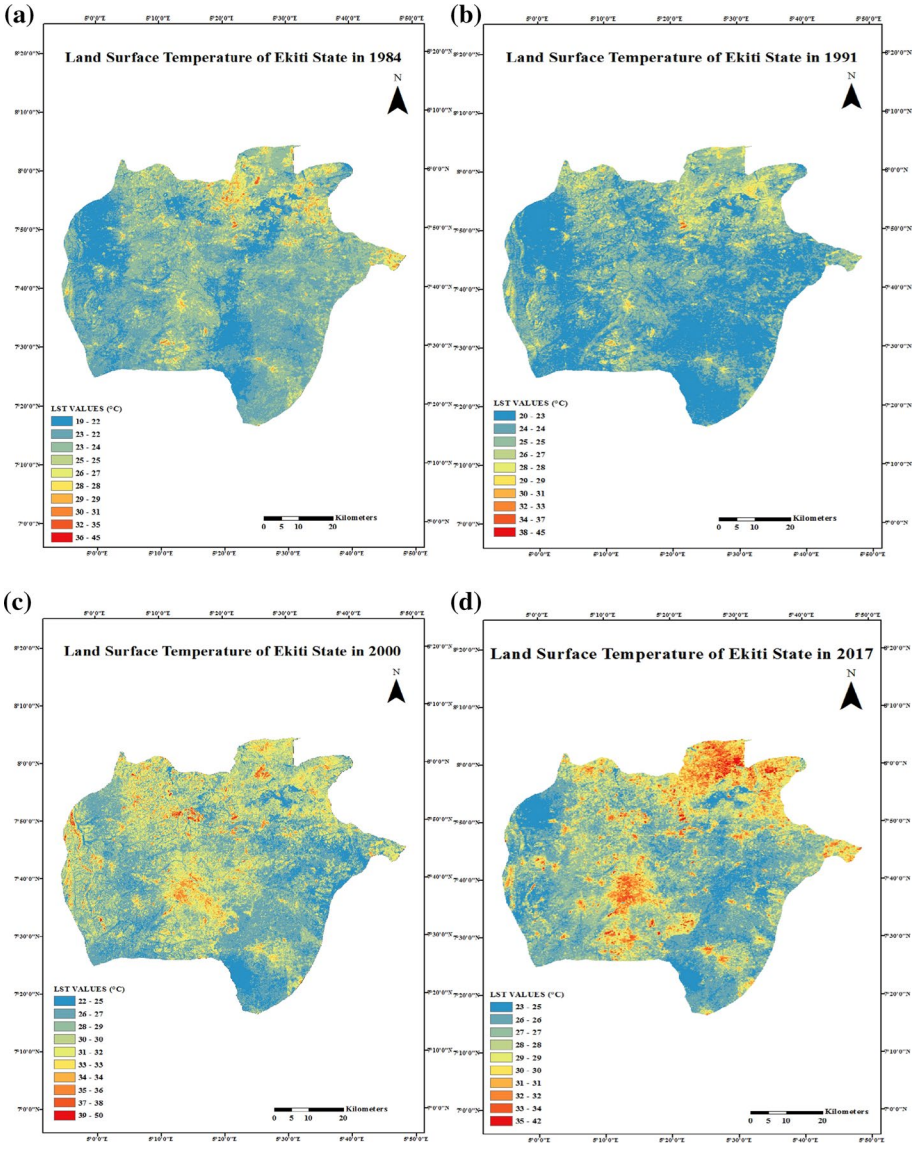

Fig. 9 LST maps of Ekiti State for the years **a** 1984, **b** 1991, **c** 2000 and **d** 2017

4 Discussion

4.1 Land use/land covers classification and changes analysis

Ekiti State which is comprised of tropical rainforest in the south and derived guinea savannah in the northern peripheries is currently witnessing its intermediate stage of development process. In 1972, the forest land cover was approximately 73.90% of the entire Ekiti State land mass. During the same period, the cropland occupied 15.85% of the State's land

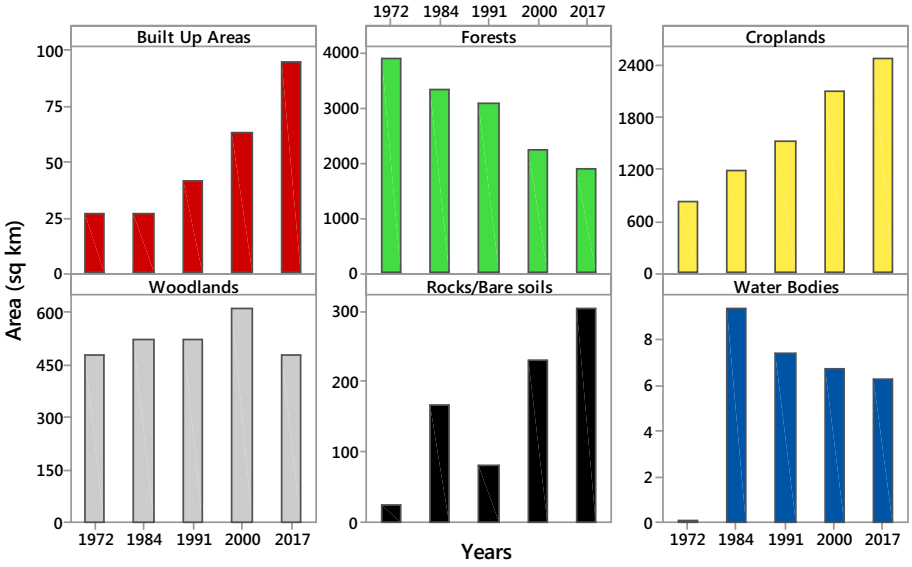

Fig. 10 LULC class change trend (sq. km) from 1971 to 2017

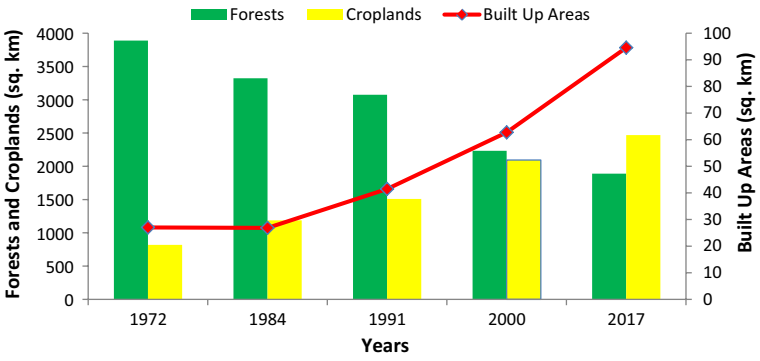

Fig. 11 Temporal pattern of urban encroachment on croplands and forest resources

area (Table 4). Area distribution changes of the LULC maps of Ekiti State show a major decline in Forest lands (i.e., from 1984 upward), whereas built-up areas, croplands, and rocks/bare soils increased (Table 5, Fig. 10). Construction of three large earth dams in the state led to the unusual increase in the coverage of water bodies extent from 1972 to 1984 (i.e., 9.35 km^2 increase). The forest covers shrank from 73.90 to 36.03% area of the LULC (Table 4) showing a total reduction of 37.87% over a period of 4 decades while the built-up areas, bare soils, and croplands increased by 1.31, 5.10 and 31.28% area of the LULC, respectively. The conversion of forests to croplands over the entire period (1972–2017) was significant, forest being the major source of land for croplands enlargement. This is an indication of significant change in the ecosystem of the state with attendant effects on its functioning and sustainability. Built-up areas and croplands had strong influence on the loss of forest land cover class between 1972 and 2017 (Fig. 11). This is not unconnected to the

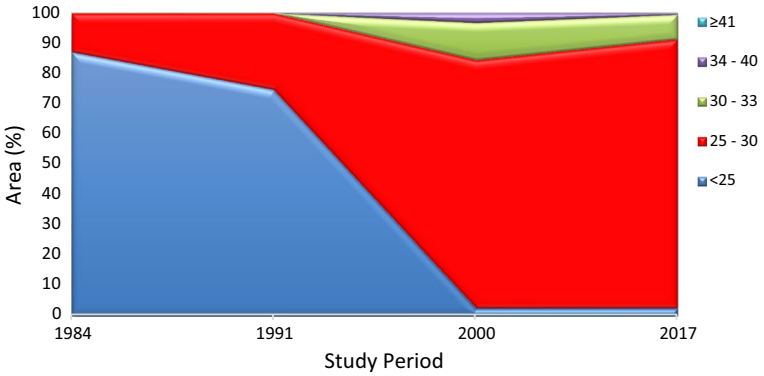

Fig. 12 LST zones for the period 1984–2017 in Ekiti State

fact that agricultural activities are the main livelihood of the people providing revenue and employment to more than 75% of the State's population (www.ekiti.com, retrieved—2018, Jan. 28). The obvious increase in the population of the state in the early 90s when the study area was officially declared a state in the southwestern geopolitical zone of Nigeria has triggered many changes in the LULC of the state. More spaces and forest resources are utilized in an increasing population (refer to Sect. 2.1) (Fig. 10). In the local contexts, population pressure, illegal logging of forest trees for timber and wood products and activities of charcoal merchants are majorly responsible for the land cover transformations witnessed in the study area. Recently, rapidly expanding business of ornate species of trees has greatly induced transition of forests in the state to other land cover types.

This pattern of forest conversion is a longstanding phenomenon both locally and globally (Meyfroidt et al. 2013; Gollnow and Lakes 2014). This conforms to the findings of Ochege and Okpala-Okaka (2017) who also asserted that more forest areas are being converted to croplands for agricultural production in South-eastern Nigeria. Likewise, proximity of the croplands to the settlements necessitated their conversion to residential and industrial areas (Ochege and Okpala-Okaka 2017). Urbanization had been widely acknowledged as one of the most widespread anthropogenic causes of the loss of arable lands (Lopez et al. 2001), and agricultural land clearing also being the major driver of habitat destruction (Alphan 2003) and decline in natural vegetation cover (Figs. 10, 11).

4.2 Land use/land covers change and sustainable environment

NDVI has been used for change detection analysis in many studies (Singh et al. 2016). A higher value of NDVI is an indication of the presence of healthy vegetation in the study area while sparse vegetation (Singh et al. 2016) and other land use and land covers infer lower NDVI value (Fig. 8). The decrease in the values of NDVI of the study area during the study period (1972–2017) could be attributed to degradation and loss of forest area mainly due agricultural expansion and anthropogenic encroachment. The result obtained in this study is similar to that of Singh et al. (2016) who reported a significant decrease in NDVI values of Lower Assam, India between 1990 and 2014. These observations are particularly important because the spatial characteristics of LULC are useful for understanding the various impacts of human activity on the overall ecological condition of the urban environment (Yeh and Li 1999). Furthermore, the moderate

values of NDVI observed in the study area from the Landsat satellite images for the years of study may have resulted from the dates of data acquisition which falls in the peak of the dry season. This is due to the fact that precipitation is the chief determinant of vegetation cover (Seboka 2016).

In time past, information on different LULC types have been extracted using LST due to its sensitivity to various land surface features (Ibrahim 2017). A progressive increase in the LST was noted in the study area during the period of observation. Figure 9 clearly shows that non-vegetated surfaces recorded the highest LST values; meanwhile, the vegetated surfaces had the lowest LST values. This condition is attributed to the cooling effects vegetation has on air temperature due to transpiration. These results suggest that the various surface features categorized as urban areas and uncultivated bare land tend to absorb heat quickly than other LULC types in the study area (Dewan and Corner 2012). The implication is that high surface temperatures were experienced over urban areas and uncultivated bare land in all the periods of study (Figs. 9, 12) due to its high heat capacity (Dewan and Corner 2012). This invariably has a marked effect on the natural functioning of ecosystems (Turner 1995). The earth landscapes and the atmosphere have been altered as a result of urbanization and other anthropogenic activities, and this has led to a changed thermal climate that is warmer in urban areas than the surrounding non-urbanized areas (Joshi and Bhatt 2012). It was observed that vegetation and water bodies have lesser LST values (between 19 and 24 °C) compared to built up, rocks and uncultivated bare soil. Several studies such as Dewan and Corner (2012) and Xiao and Weng (2007) have examined the effect of land use/land cover change on LST and found a positive correlation between LST and the impervious surface. Likewise, Pal and Ziaul (2015) reported significant LST variations over various LULC types in English Bazar Municipality of Malda District in West Bengal, India. This further verified that LST varies in response to the surface energy balance and equally modulates the air temperature of the lowest layers of the urban atmosphere (Voogt and Oke 2003). In recent years, the concentration of thermal environment has increased including greenhouse effect and global warming; referring to the air temperature and the LST (Rehman et al. 2016). As the warmth rising off Earth's landscapes effects (and is also being influenced by) our world's weather and climate patterns, sustained monitoring of the LST is vital (earthobservatory.nasa.gov, retrieved—2018, March. 12). LST monitoring is of primarily important in a variety of fields such as vegetation monitoring, evapotranspiration, hydrological cycle, climate change, urban climate and environmental studies etc. (Li et al. 2013). Also, LST provide information on the spatiotemporal variations of the surface equilibrium state (Li et al. 2013). Effects of increasing atmospheric gases on LST and how rising LST, in turn, affects vegetation in Earth's ecosystems is a top priority among Scientists.

The changes in LST shown Fig. 12 have serious environmental implications in the study area, entire Country and the world at large as seen in the changes of the local and regional climate. These changes initially may seem to be localized, but on the long run contribute to the global heat (Joshi and Bhatt 2012). Along with other sorts of pollutants, United Nations (2010) predicted a rapid increase in land surface temperature which will expose expectedly 69% of the world population by 2050 to this vulnerability (United Nations 2010). In recent times, heat waves have been experienced in some parts of the country probably due to increased land surface temperature and trapped excess heat. With the excess trapped heat resulting from decreased vegetation and increased impervious surfaces and bare lands, holistic approach is needed to promote sustainable growth and development.

4.3 Relationships between LST and NDVI

Correlation and regression analysis were used to investigate and model the relationships between LST and NDVI (Fig. 13). In the present study, LST showed negative correlation with NDVI ($r = -0.672$). The regression model explained 44.77% of the variation in land surface temperature. The linear model indicates that when NDVI increases, there is a decrease in the values of LST. Thus, when the NDVI value decreased by 1 unit (due to loss of forest cover), the land surface temperature increased by 11.41 units. The negative correlation between land surface temperature and NDVI is due to the cooling effect of green areas (i.e., vegetation) on the temperature of the area. Inverse relationship of such has been reported between LST and NDVI in previous studies and it has been concluded that vegetation can lower the land surface temperature (Weng 2001). The relationship between LST and NDVI is not statistically significant ($p > 0.05$), which might be due to small sample size. However, there exist a marginal evidence of relationship between LST and NDVI that may be worth further exploration, perhaps with a larger sample.

The benefits, humankind derive from the natural functioning of a healthy and productive vegetation system, are constantly being threatened by rapid modification of the land cover classes (Table 6). Apart from the provision of the basic needs of life (i.e., food, clothing, and shelter), the natural vegetation enables purification of water bodies (Friberg et al. 2011), regulates climate and the functioning of the biosphere (Millennium Ecosystem Assessment 2005) preventing pollution and climate change. With an estimated 50% of the global population living in urban areas, and with this percentage expected to reach 69.6% by 2050 (United Nations 2010), the natural vegetation is

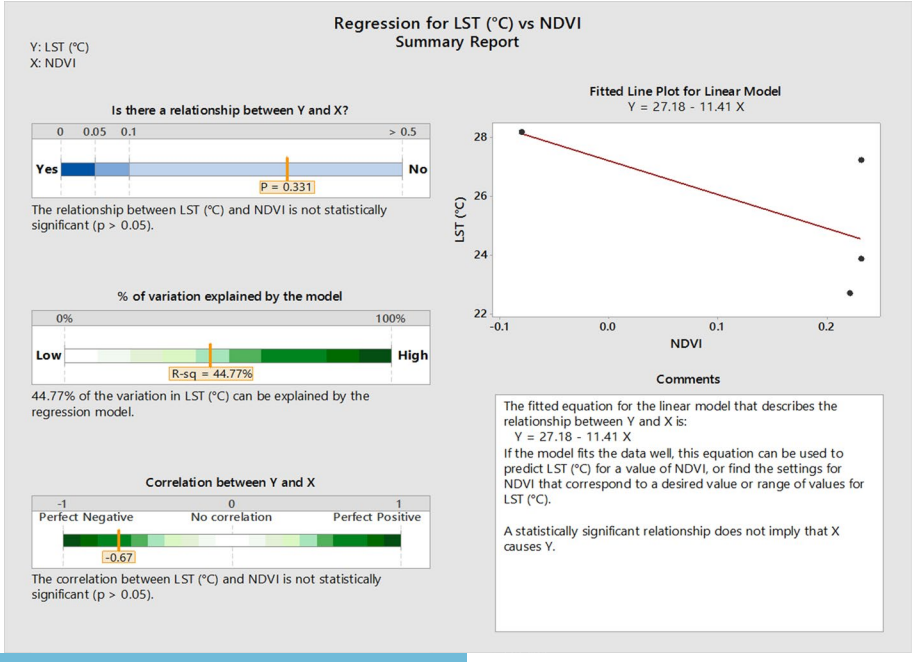

Fig. 13 Correlation plot for LST and NDVI

under significant risk of conversion to impervious surfaces and bare lands. The loss of natural vegetation and the increase of impermeable non-transpiring, non-evaporating hard land surfaces resulted to increasing surface temperatures (LST), a foremost crucial problem facing the non-vegetated areas (Hussain et al. 2014). As such, urban dwellers are confronted with diverse ecological problems (increased surface energy; anthropogenic heat discharge; building energy consumption; atmospheric pollution; and thermal stress) (Sarrat et al. 2006). This is a common global scenario, especially, with regard to reduction in evapotranspiration, promotion of more rapid surface runoff, increased storage and transfer of sensible heat, and reduction of air and water quality (Wilson et al. 2003). Likewise, increased heat waves, unhealthy vegetation and ecosystem (reduced highest NDVI values down the years), and global warming, etc. are common circumstance. These negatively affect the landscape esthetics, energy efficiency, human health and quality of living in non-vegetated environments are the resultant effects of these alterations (Mcpherson et al. 1997).

5 Conclusion

This study evaluated the land use/land cover dynamics of Ekiti State, southwestern Nigeria in the past four and half decade. It also evaluated the spatial distribution of normalized difference vegetation index and land surface temperature distribution of the study area. Significant changes in the land use/land cover of the study area were observed during the study period. The rapidly growing population of the study area has resulted to increasing demand for living spaces and forest resources. The study has shown that forests shrunk by 37.87% (i.e., 1983.95 sq km) mainly because of agricultural expansion and expansion of built-up areas. Croplands exerted a strong influence on the loss of forest cover recorded in the study area over the last four and half decades. Deforestation and forests degradation observed during the study period has triggered immense loss of several indigenous trees and forests which has accentuated the depletion of the state's forestry resources and several species extinction. Population pressure, illegal logging of forest trees for timber and wood products and activities of charcoal merchants are the major drivers of deforestation in the state. Decreased in NDVI values resulted from widespread deforestation and forest degradation, while higher absorption of solar radiation and greater thermal capacity associated with urban surfaces such as buildings, roads, and other paved surfaces could led to increased LST of the study area. Presence of vegetations in urban areas can reduce the high thermal capacity due to the cooling effects vegetation has on air temperature as a result of transpiration. These observations are particularly important because the spatial characteristics of LULC are useful for understanding the various impacts of human activity on the overall ecological condition of the urban environment. A study of land use systems and practices is useful in appreciating the challenges and prospects of sustainable development. Thus, an initiative to provide more space for greening and reducing land surface temperature is a must in urban development. Remote sensing and GIS have proven to be useful tools in the understanding of the earth systems and has equally provided vital information in preserving it.

Acknowledgements The authors express gratitude to the United States Geological Survey (USGS) for assisting this research with datasets. We are also indebted to the handling editor and the three anonymous reviewers for their comments which significantly improved the quality of the manuscript.

Compliance with ethical standards

Conflicts of interest The authors declare that they have no conflict of interest.

References

Adeel, M. (2010). Methodology for identifying urban growth potential using land use and population data: A case study of Islamabad zone IV. *Procedia Environmental Sciences, 2,* 32–41.

Al-doski, J., Mansor, S. B., & Shafri, H. Z. M. (2013). NDVI differencing and post classification to detect vegetation changes in Halabja City, Iraq. *IOSR-JAGG, 1*(2), 01–10.

Alphan, H. (2003). Land use change and urbanization in Adana, Turkey. *Land Degradation and Development, 14*(6), 575–586.

Artis, D. A., & Carnahan, W. H. (1982). Survey of emissivity variability in thermography of urban areas. *Remote Sensing of the Environment, 12,* 313–329.

Babalola, O. S., & Akinsanola, A. A. (2016). Change detection in land surface temperature and land use land cover over Lagos Metropolis, Nigeria. *Journal of Remote Sensing and GIS, 5,* 171. https://doi.org/10.4172/2469-4134.1000171.

Butt, A., Shabbir, R., Ahmad, S. S., & Aziz, N. (2015). Land use change mapping and analysis using Remote Sensing and GIS: A case study of Simly watershed, Islamabad, Pakistan. *The Egyptian Journal of Remote Sensing and Space Sciences, 18,* 251–259.

Demessie, E. T. (2015). Soil hydrological impacts and climatic controls of land use and land cover changes in the Upper Blue Nile (Abay) basin. Delft University of Technology, The Netherlands and the Academic Board of the UNESCO-IHE. CRC Press/Balkema, P. O. Box 11320, 2301 EH Leiden, The Netherlands. ISBN: 978-1-138-02874-6 (Taylor & Francis Group)

Denman, K. L., Brasseur, G. A., Chidthaisong, P., Ciais, P. M., Cox, R. E., Dickinson, D., et al. (2007). The Physical science basis. In S. Solomon (Ed.), *Climate change 2007* (pp. 663–745). Cambridge: Cambridge University Press.

Dewan, A. M., & Corner, R. J. (2012). The impact of land use and land cover changes on land surface temperature in a rapidly urbanizing megacity. IEEE. ISBN 978-1-4673-1159-5/12/$31.00

Eastman, J. R. (2016). *TERRSET Tutorial. Clark labs, Clark University, Worcester*. http://www.clarklabs.org.Ekiti. Accessed March 6, 2018.

Ekiti (State, Nigeria)—Population Statistics, Charts, Map and Location. (2018). Retrieved from http://www.citypopulation.de/php/nigeria-admin.php?adm1id=NGA013.

FAO. 1998. World reference base for soil resources, by ISSS–ISRIC–FAO. World Soil Resources Report No. 84. Rome.

FAO/UNEP. (1999). *Terminology for integrated resources planning and management*. Rome, Italy and Nairobi, Kenya: Food and Agriculture Organization/United Nations Environmental Program.

Friberg, N., Bonada, N., Bradley, D. C., Dunbar, M. J., Edwards, F. K., Grey, J., et al. (2011). Biomonitoring of human impacts in freshwater ecosystems: The good, the bad and the ugly. *Advances in Ecological Research*. https://doi.org/10.1016/B978-0-12-374794-5.00001-8.

Gollnow, F., & Lakes, T. (2014). Policy change, land use, and agriculture: The case of soy production and cattle ranching in Brazil, 2001–2012. *Applied Geography, 55,* 203–211.

Hegazy, I. R., & Kaloop, M. R. (2015). Monitoring urban growth and land use change detection with GIS and remote sensing techniques in Daqahlia governorate Egypt. *International Journal of Sustainable Built Environment, 4,* 117–124.

Higginbottom, T. P., & Symeonakis, E. (2014). Assessing land degradation and desertification using vegetation index data: Current frameworks and future directions. *Remote Sensing, 6,* 9552–9575. https://doi.org/10.3390/rs6109552.

History of Ekiti State. (2018). Retrieved from logbaby.com/encyclopedia/history-of ekiti-state_10026.html#.Wynq9FVKgdU https://phenology.cr.usgs.gov/ndvi_foundation.php. Accessed February 10, 2018.

Hussain, A., Bhalla, P., & Palria, S. (2014). Remote sensing-based analysis of the role of land use/land cover on surface temperature and temporal changes in temperature: A case study of Ajmer District, Rajasthan. *The International Archives of Photogrammetry, Remote Sensing and Spatial Information Sciences, 8,* 1447–1454.

Ibrahim, G. R. F. (2017). Urban land use land cover changes and their effect on land surface temperature: Case study using Dohuk City in the Kurdistan Region of Iraq. *Climate, 5,* 13. https://doi.org/10.3390/cli5010013.

IPCC. (2013). Summary for policymakers. In T. F. Stocker, D. Qin, G. K. Plattner, M. Tignor, S. K. Allen, J. Boschung, A. Nauels, Y. Xia, V. Bex, & P. M. Midgley (Eds.), *Contribution of working groups I to the fifth assessment report of the intergovernmental panel on climate change* (p. 27). Cambridge: Cambridge University Press.

Iqbal, M. F., & Khan, I. F. (2014). Spatiotemporal land use land cover change analysis and erosion risk mapping of Azad Jammu and Kashmir, Pakistan. *The Egyptian Journal of Remote Sensing and Space Sciences, 17,* 209–229.

Ishola, K. A., Okogbue, E. C., & Adeyeri, O. E. (2016). Dynamics of surface urban biophysical compositions and its impact on land surface thermal field. *Modeling Earth System and Environment, 2,* 208. https://doi.org/10.1007/s40808-016-0265-9.

Joshi, J. P., & Bhatt, B. (2012). Estimating temporal land surface temperature using remote sensing: A study of Vadodara Urban Area, Gujarat. *International Journal of Geology, Earth and Environmental Sciences, 2*(1), 123–130. ISSN: 2277-2081.

Kantakumar, L. N., & Neelamsetti, P. (2015). Multi-temporal land use classification using hybrid approach. *The Egyptian Journal of Remote Sensing and Space Sciences, 18,* 289–295.

Kasischke, E. S., Goetz, S., Hansen, M. C., Ozdogan, M., Rogan, J., Ustin, S., et al. (2004). Temperate and boreal forests. In S. Ustin (Ed.), *Manual of remote sensing. Vol. 4: Remote sensing for natural resource management and environmental monitoring*. New York: Wiley.

Kuenzer, C., & Dech, S. (2013). *thermal infrared remote sensing: sensors, methods, applications*. London: Springer.

Landsat Project Science Office. (2002). Landsat 7 Science Data User's Handbook. http://ltpwww.gsfc.nasa.gov/IAS/handbook/handbook_toc.html, Goddard Space Flight Center, NASA, Washington, DC (last date accessed September 10, 2003).

Lea, C., & Curtis, A. C. (2010). Thematic accuracy assessment procedures: National Park Service Vegetation Inventory, version 2.0. Natural Resource Report NPS/2010/NRR 2010/204, National Park Service, Fort Collins, Colorado, USA.

Li, Z., Tang, B., Wu, H., Ren, H., Yan, G., Wan, Z., Trigo, I. F., & Sobrino, J. A. (2013). Satellite derived land surface temperature: Current status and perspectives. *Remote Sensing of Environment, 131,* 14–37.

Lillesand, T. M., & Kiefer, R. W. (2007). *Remote sensing and image interpretation* (5th ed., p. 820). New York: Wiley.

Lopez, E., Bocco, G., Mendoza, M., & Duhau, E. (2001). Predicting land cover and land use change in the urban fringe a case in Morelia City, Mexico. *Landscape and Urban Planning, 55*(4), 271–285.

Magidi, J. T. (2010). Spatio-temporal dynamics in land use and habitat fragmentation in the sandveld, South Africa. MSc thesis, Department of Biodiversity and Conservation Biology, University of the Western Cape, Western Cape.

Mallick, J., Kant, Y., & Bharath, B. D. (2008). Estimation of land surface temperature over Delhi using-Landsat-7 ETM+. *Journal of Indian Geophysical Union*, *12*(3), 131–140.

Markham, B. L., & Barker, J. L. (1985). Spectral characterization of the landsat thematic mapper sensors. *International Journal of Remote Sensing, 6*(5), 697–716.

Mcpherson, E. G., Nowak, D., Heisler, G., Grimmond, S., South, C., Grant, R., et al. (1997). Quantifying urban forest structure, function, and value: The Chicago urban forest climate project. *Urban Ecosystems, 1,* 49–61.

Mengistu, D. A., (2008). Remote sensing and gis-based Land use and land cover change detection in the upper Dijo river catchment, Silte zone, southern Ethiopia. Working papers on population and land use change in central Ethiopia, nr. 17 Acta Geographica-Trondheim Serie A, Nr. 23 Series A, No. 23.

Meyfroidt, P., Lambin, E. F., Erb, K., & Hertel, T. W. (2013). Globalization of land use: Distant drivers of land change and geographic displacement of land use. *Human Settlements and Industrial Systems, 5*(5), 438–444.

Millennium Ecosystem Assessment. (2005). *Ecosystems and human well-being: synthesis*. Washington, DC: Island Press.

Minta, M., Kibret, K., Thorne, P., Nigussie, T., & Nigatu, L. (2018). Land use and land cover dynamics in Dendi-Jeldu hilly-mountainous areas in the central Ethiopian highlands. *Geoderma, 314,* 27–36.

Mohamed, N. A. H., Salih, E. M., & Abdu, A. S. (2011). Monitoring vegetation degradation as indicator of desertification in sudan using NDVI data (1993–2003). *Sudan Journal Desert Research, 3*(1), 15–27.

Muttitanon, W., & Tripathi, N. (2005). Land use/cover changes in the coastal zone of Bay Don Bay, Tailand using Landset 5 TM data. *International Journal of Remote Sensing, 26*(11), 2311–2323.

National Bureau of Statistics (NBS). (2012). Annual abstract of statistics. Federal Republic of Nigeria. https://www.nigerianstat.gov.ng. Accessed February 7, 2018.

Ochege, F. U., & Okpala-Okaka, C. (2017). Remote sensing of vegetation cover changes in the humid tropical rainforests of Southeastern Nigeria (1984–2014). *Cogent Geoscience, 3,* 1307566.
Ogundare, B. A. (2016). A comparative analysis of agricultural land use in Ikere Ekiti, Nigeria. *An International Peer-reviewed Journal*, *27*, 1–6.
Olorunfemi, I. E. (2014). Occurrence, causes, and impacts of hydrophobicity on soils of different land uses in Ekiti State. M.Eng. thesis. Federal University of Technology, Akure, Nigeria.
Olorunfemi, I. E., & Fasinmirin, J. T. (2017). Land use management effects on soil hydrophobicity and hydraulic properties in Ekiti State, forest vegetative zone of Nigeria. *CATENA, 155,* 170–182.
Olorunfemi, I. E., Fasinmirin, J. T., & Akinola, F. F. (2018). Soil physico-chemical properties and fertility statusof long-term land use/land cover changes A case study in Forest vegetative zone of Nigeria. *EurasianJournal of Soil Science*, *7*(2), 133–150.
Omran, E. E. (2012). Detection of land-use and surface temperature change at different resolutions. *Journal of Geographic Information System, 4,* 189–203.
Owojori, A., & Xie, H. (2005). Landsat image-based LULC changes of San Antonio, Texas using advanced atmospheric correction and object-oriented image analysis approaches. Paper Presented at the 5th international symposium on remote sensing of Urban Areas, Tempe, AZ.
Pal, S., & Akoma, O. C. (2009). Water scarcity in wetland area within Kandi Block of West Bengal: A hydrological assessment. *Ethiopia Journal of Environmental Studies and Management, 2*(3), 1–12.
Pal, S., & Ziaul, S. K. (2015). Detection of land use and land cover change and land surface temperature in English Bazar urban centre. *The Egyptian Journal of Remote Sensing and Space Sciences, 20,* 125–145.
Population Figures. (2018). Retrieved from http://ekitistate.gov.ng/about-ekiti/populationfigures/. Accessed February 6, 2018.
Rawat, J. S., Biswas, V., & Kumar, M. (2013). Changes in land use/cover using geospatial techniques: a case study of Ramnagar town area, district Nainital, Uttarakhand, India. *The Egyptian Journal of Remote Sensing and Space Sciences, 16,* 111–117.
Rawat, J. S., & Kumar, M. (2015). Monitoring land use/cover change using remote sensing and GIS techniques: a case study of Hawalbagh block, district Almora, Uttarakhand, India. *The Egyptian Journal of Remote Sensing and Space Sciences, 18,* 77–84.
Rehman, Z., Khanum, F., & Kazmi, S. J. H. (2016). Evaluation of land cover changes at the coast of Sindh through successive landsat imageries. *Earth Science and Climatic Change, 7,* 325. https://doi.org/10.4172/2157-7617.1000325.
Rouse, J. W., Haas, R. H., Schell, J. A., & Deering, D. W. (1974). Monitoring the vernal advancement and retrogradation (green wave effect) of natural vegetation. Final Report. RSC 1978-4. Remote Sensing Center, Texas A&M University, College Station.
Sarrat, C., Lemonsu, A., Masson, V., & Guedalia, D. (2006). Impact of urban heat island on regional atmospheric pollution. *Atmospheric Environment, 40,* 1743–1758.
Seboka, G. N. (2016). Spatial assessment of NDVI as an indicator of desertification in ethiopia using remote sensing and GIS. Master degree thesis, Master in Geographical Information Science Department of Physical Geography and Ecosystem Science, Lund University.
Shalaby, A., & Tateishi, R. (2007). Remote sensing and GIS for mapping and monitoring land cover and land-use changes in the Northwestern coastal zone of Egypt. *Applied Geography, 27*(1), 28–41.
Simon-Oke, O., Jegede, O., & Osamede, A. (2012). Spatial distribution of micro finance institutions and agricultural development in Ekiti State, Nigeria. *AFRREV IJAH: An International Journal of Arts and Humanities, 1*(3), 258–269.
Singh, R. P., Singh, P., Singh, S., & Mukherjee, S. (2016). Normalized difference vegetation index (NDVI) based classification to assess the change in land use/land cover (LULC) in Lower Assam, India. *International Journal of Advanced Remote Sensing and GIS, 5*(10), 1963–1970.
Smyth, A. J., & Montgomery, R. F. (1962). *Soil and Land use in central Western Nigeria* (p. 265). Ibadan: Govt. Printer.
Turner, H. B. L. (1995). Linking the Natural and Social Sciences. The land use/cover change core project of International Geosphere-Biosphere Programme (IGBP). IGBP Newsletter, No. 22.
United Nations. (2010). World urbanization prospects: The 2009 revision population database. http://esa.un.org/unpd/wup/index.htm. Accessed February 17, 2018.
Veldkamp, A., & Lambin, E. F. (2001). Predicting land use change. *Agriculture, Ecosystem and Environment, 85,* 1–6.
Veldkamp, A., & Verburg, P. H. (2004). Modelling land use change and environmental impact. *Journal of Environment Management, 72,* 1–2.
Voogt, J. A., & Oke, T. R. (2003). Thermal remote sensing of urban climates. *Remote Sensing of Environment, 86,* 370–384. https://doi.org/10.1016/S0034-4257(03)00079-8.

Wang, S., Xu, J., & Zhou, C. (2002). Using remote sensing to estimate the change of carbon storage: A case study in the estuary of Yellow River delta. *International Journal of Remote Sensing, 23*(8), 1565–1580.

Wei, H., Qiping, G., Wang, H., & Hong, J. (2015). Simulating land use change in urban renewal areas: A case study in Hong Kong. *Habitat International, 46,* 23–34. https://doi.org/10.1016/j.habitatint.2014.10.008.

Weng, Q. (2001). A remote sensing? GIS evaluation of urban expansion and its impact on surface temperature in the Zhujiang Delta, China. *International Journal of Remote Sensing, 22*(10), 1999–2014.

Wilson, J. S., Clay, M., Martin, E., Stuckey, D., & Risch, K. V. (2003). Evaluating environmental influence of zoning in urban ecosystems with remote sensing. *Remote Sensing of Environment, 86,* 303–321.

Xiao, H. L., & Weng, Q. H. (2007). The impact of land use and land cover changes on land surface temperature in a karst area of China. *Journal of Environmental Management, 85,* 245–257.

Yeh, A. G. O., & Li, X. (1999). Economic development and agricultural land loss in the Pearl River Delta, China. *Habitat International, 23,* 373–390.

Yuan, D., Elvidge, C. D., & Lunetta, R. S. (1998). Survey of multispectral methods for land cover change analysis. In R. S. Lunetta & C. D. Elvidge (Eds.), *Remote sensing change detection. Environmental monitoring methods and applications* (pp. 21–39). Chelsea, MI: Ann Arbor Press.

Zubair A.O. (2006). Change detection in land use and Land cover using remote sensing data and GIS: A case study of Ilorin and its environs in Kwara State. MSc. thesis, University of Ibadan, Nigeria.